Biotemplates for Nanotechnology

DOI: 10.1002/anie.200801802

Fungal Templates for Noble-Metal Nanoparticles and Their Application in Catalysis**

*Nadja C. Bigall, Manuela Reitzig, Wolfgang Naumann, Paul Simon, Karl-Heinz van Pée, and Alexander Eychmüller**

The combination of living structures with advanced materials, for example, as realized in cell–semiconductor coupling,[1] or by using small biological forms as templates for nanotechnological applications, is becoming the focus of more and more interest. Composite materials consisting of magnetic or semiconducting nanoparticles incorporated into bacterial superstructures have been synthesized.[2] To date, the main work on nanoparticle biomaterial hybrid structures has been done using functionalized gold nanoparticles assembled onto bacteria. For example Berry et al. were able to synthesize highly electrically conducting materials by assembling lysine-coated gold nanoparticles onto *Bacillus cereus*.[3] It has also been demonstrated that cetyltrimetylammonium bromide (CTAB) terminated gold nanoparticles of different shapes (for example, nanorods) can be assembled onto the surface of bacteria.[4] Other techniques for controlled assembly of gold nanoparticles were performed by DNA-modification of the surface, using diatoms and fungi as templates.[5] Very recently Sugunan et al. reported the growth of fungi directly in gold nanoparticle solutions, using sodium glutamate as the reducing agent.[6] Nutrition-driven assembly of gold onto the fungal mycelia was detected. The resulting hybrid structure exhibited optical properties of bulk gold and an electric resistivity close to that of the respective bulk solid.

In this article we show the ability of a variety of fungi to grow in citrate-stabilized colloidal medium and test their affinity for different noble-metal nanoparticles. Fungal growth takes place directly in the as-prepared gold, silver, platinum, and palladium nanoparticle solutions. Decoration of the fungal surface takes place without any further functionalization. The resulting hybrid systems have outer dimensions of about 0.1 cm^3 and optical properties similar to the respective nanoparticle solutions. Differences in the metal affinities with respect to the morphology were observed by scanning electron microscopy. The specific surface area of the systems obtained has been assessed. A fungus–platinum hybrid system was shown to catalyze the redox reaction of hexacyanoferrate(III) and thiosulfate ions in aqueous solution. Dehydration of the metal–fungus hybrids was performed by critical point drying, thus conserving the three-dimensional macroscopic and microscopic shapes.

Besides the potential for applications in heterogeneous catalysis, other applications for these hybrid structures can also be considered. Silver or gold structures could be used as templates for surface-enhanced Raman spectroscopy and might also serve for fungi identification.[7] Fungi decorated with silver could serve as disinfecting objects because of their high porosity and the well-known disinfection capability of silver. Besides electronic or sensoric applications, the effect described could be a useful tool for biochemical investigations, for example concerning the fungal heavy-metal-accumulation effect or for detecting differences in surface modifications (for example, between spores and hyphae).

Figure 1 displays the absorption spectra of the metal nanoparticle solutions without any further dilution. The absorbances of palladium and platinum do not show any significant maxima, whereas the absorption maximum originating from the plasmon excitation of the colloidal gold is at 524 nm. The very distinct plasmon peak of the silver nanoparticles is at 402 nm.

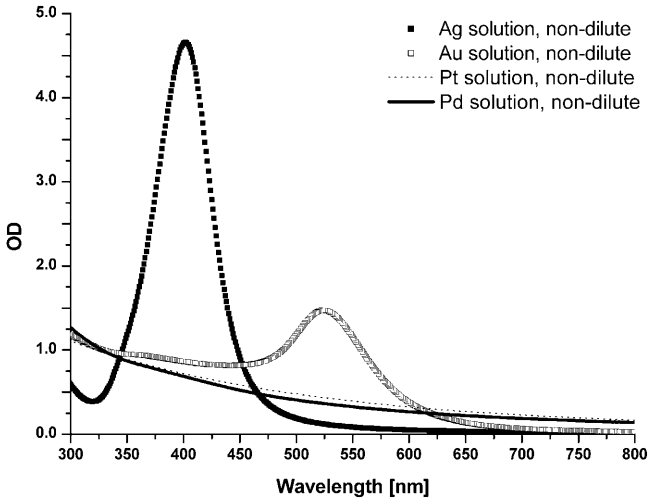

Figure 1. Absorption spectra of the as-prepared nanoparticle solutions. The metal nanoparticles were synthesized in aqueous media at 100 °C and with the same precursor concentrations in all cases.

[*] N. C. Bigall, Prof. A. Eychmüller
Physical Chemistry, TU Dresden
Bergstrasse 66b, 01062 Dresden (Germany)
Fax: (+49) 351-463-37164
E-mail: alexander.eychmueller@chemie.tu-dresden.de
Homepage: http://www.chm.tu-dresden.de/pc2/
M. Reitzig, Dr. W. Naumann, Prof. K.-H. van Pée
Biochemistry, TU Dresden
Bergstrasse 66, 01062 Dresden (Germany)
Dr. P. Simon
Chemical Physics of Solids, MPI
Nöthnitzer Strasse 40, 01187 Dresden (Germany)

[**] The authors thank Ellen Kern for the SEM measurements and Dr. Dirk Dorfs and Dr. Stephen G. Hickey for fruitful discussions. We also thank Prof. Dr. Hannes Lichte for the possibility to perform TEM measurements at the Triebenberg Laboratory.

Supporting information for this article is available on the WWW under http://dx.doi.org/10.1002/anie.200801802.

Mean particle diameters of 4 nm for Pd, 5 nm for Pt, 8 nm for Ag, and 23 nm for Au nanoparticles were obtained from TEM images (see Supporting Information). Information about the crystallinity and lattice constants were obtained from high-resolution TEM images, as shown in the Supporting Information. The four batches synthesized consisted of crystalline nanoparticles. Polycrystalline structures consisting of lattice domains were mainly detected for gold and silver nanoparticles. The lattice constants obtained from HRTEM were compared with reported values and found to correspond to the (111)-plane distances of the respective bulk materials.

The left photograph in Figure 2 shows *Penicillium citreonigrum* grown in a colloidal gold solution for three months (see Supporting Information). A photograph of a similarly treated gold–fungus hybrid structure after critical point drying is shown in Figure 2 (right-hand side). This sample had an outer volume of about 0.07 cm^3 and a total mass of 0.50 mg, so that we were able to attribute an average density of approximately 7 $mg\,cm^{-3}$.

Figure 2. Color photographs of a gold-*Penicillium citreonigrum* hybrid structure in a gold nanoparticle solution (left), and after critical point drying (right).

A scanning electron micrograph taken in the backscattering mode of a typical structure is depicted in Figure 3. The bright areas correlate with a high electron density and thus indicate a significant amount of gold. Remarkably, the morphology of the underlying mycelium structure acting as the template for the gold particles is still recognizable. The micrograph on the right of Figure 3 has been detected with a higher resolution from the marked area on the left of Figure 3. From the broken gold–hyphae hybrid it is possible to get an impression of the thickness of this structure. Apparently, the gold shell has a thickness of about 0.2 μm. As the gold particles in this case had mean diameters of ten to twenty nanometers (see Supporting Information), there is evidence of multiple layers of nanoparticles in this case. Additionally, as the colors of the gold–fungus hybrid structures varied from pink to reddish-brown, we have evidence that the nanoparticles are still separated within the hybrid system (see Figure 2 and Supporting Information). This assumption could be confirmed by higher resolution SEM in the case of gold (see Supporting Information).

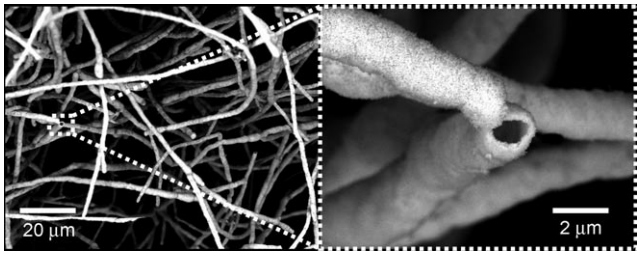

Figure 3. Left: scanning electron micrograph taken in the backscattering mode of a critical point dried gold-*Penicillium citreonigrum* hybrid structure after several months of growth, gold appears as bright areas. Right: enlargement of the area indicated, showing the hollow character of the hybrid structure.

Assuming a tubular shape of these hybrids, we were able to estimate (on the example of T07AS, see Supporting Information) a specific outer surface of about 0.4 m^2 per gram of the hybrid material. However, it must be taken into account that the approximations did not consider the additional roughness of the assembled nanoparticles so that we expect the real specific surface to be larger.

Although the same metal nanoparticle samples were used for all different fungi, the affinity of the fungi to the nanoparticles varied drastically for the gold sol (Figure 4).

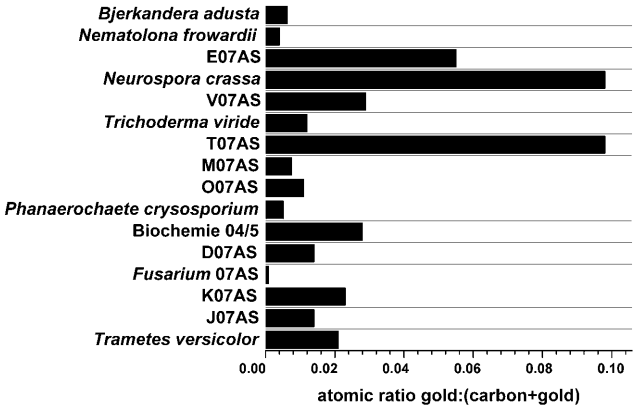

Figure 4. Graph showing the gold contents of different fungi grown under the same conditions. The atomic ratios of carbon: (carbon+gold) were obtained from EDX measurements at 500× amplification.

The graph shows that the gold content of the samples, as obtained from energy-dispersive X-ray (EDX) spectroscopic analysis, varied by up to a factor of 60. As these are all hybrid structures from the same sample of nanoparticles and the fungi had equivalent growth conditions, this difference in occupation can only be attributed to differences of the fungal surfaces or metabolic characteristics. This interesting result will be further investigated in our future work as it could be a useful tool for microbiological investigations.

We also found variations in the accumulation of the metal nanoparticles on fungi exhibiting different morphologies (Figure 5). Whereas in the case of E07AS (Figure 5, top), spores and hyphae are recognizable in both electron microscopy modes, indicating gold coverage in both morphologies, the SEMs of the fungus O07AS (Figure 5, bottom) give evidence of drastic differences in the surface of spores and hyphae since the spores are not recognizable in the gold-sensitive backscattering mode.

Most of the fungi grew best in gold, followed by platinum and palladium nanoparticle solutions. Growth of fungi in

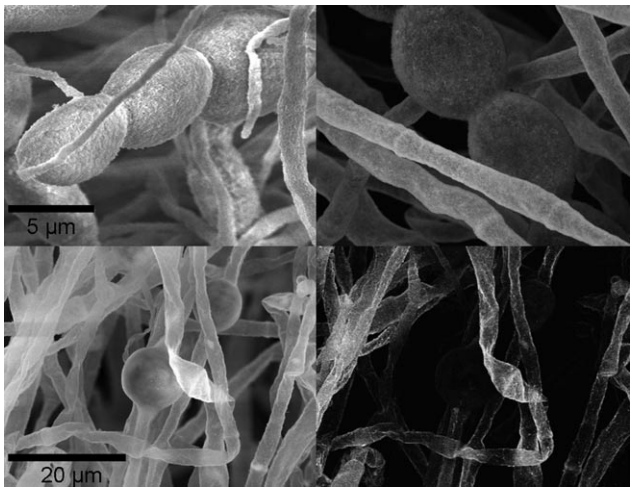

Figure 5. Scanning electron micrographs of similar regions within a hybrid structure (left: secondary electron mode, right: backscattering mode). The spores of the fungus E07AS (upper images) show significant assembly of gold nanoparticles, whereas the spores of the fungus O07AS (lower images) do not.

silver nanoparticle solution only occurred in the case of *Bjerkandera adusta*. The fact that *Bjerkandera adusta* grew in silver nanoparticle solutions is surprising, as silver is toxic to microorganisms.

The metal content of the isolated hybrid structures (as obtained from EDX measurements) from an experiment with *Trichoderma viride*, *Penicillium citreonigrum*, *Neurospora crassa*, *Bjerkandera adusta*, and three other fungi in gold, palladium, platinum, and silver nanoparticle solutions (synthesized with the same concentrations of the precursors) are displayed in the diagram in Figure 6 (right). In the backscattering mode SEM (left) palladium nanoparticles or their agglomerates are visible on the mycelia.

To investigate whether the assembled nanoparticles still had catalytically active sites, a fungus (T07AS), which had been grown in a platinum nanoparticle solution and had an atomic ratio of 0.03 for platinum:(platinum+carbon), was added to a reaction mixture of hexacyanoferrate(III) and thiosulfate (Figure 7). The use of gold or platinum nanoparticle solutions as catalysts for this reaction has already been reported by other groups.[8] The difference between the concentration curves with and without fungus is small in comparison to the case of the platinum-containing hybrid structure (Figure 7). From this graph it is clearly visible that the platinum nanoparticles retain their catalytic ability when assembled onto the fungus.

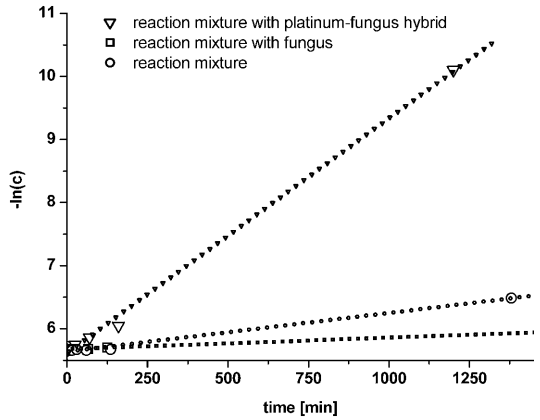

Figure 7. Time-dependent concentration of hexacyanoferrate(III) in the presence of a platinum-fungus (T07AS) hybrid system (▽), in the presence of the same fungus without platinum (□) and of the pure solutions (○) and respective interpolation curves. In the experiment 1.2 mL of 0.005 M potassium hexacyanoferrate(III) and 0.6 mL of 0.1 M sodium thiosulfate were mixed and shaken at 25 °C.

In summary, we have demonstrated the possibility of fungal growth directly in as-prepared citrate-stabilized nanoparticle solutions. Presumably, residual citrate molecules from the synthesis of the metal nanoparticles[9] are used for growth by the fungus. The decoration of the fungal surface takes place without any further functionalization. All fungi examined exhibit the ability to accumulate nanoparticles on their surfaces. Different fungi show differences in affinity to the metal nanoparticles. Solutions of gold, platinum, palladium and silver nanoparticles could be used as media for fungal growth leading to the assembly of metal particles on the living entity. The growth behavior of different fungi depended on the kind of noble-metal nanoparticles in solution.

The resulting hybrid structures exhibited the typical colors of the respective nanoparticle solutions. Therefore, we would expect a different conduction mechanism than for the systems which were obtained from fungal growth in gold sol reduced by glutamate, resulting in ohmic behavior close to bulk gold.[6]

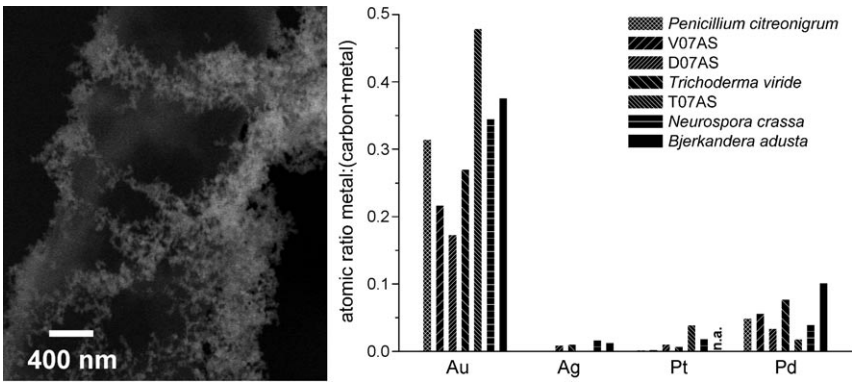

Figure 6. Left: SEM (backscattering mode) of a fungus (V07AS) grown in a palladium nanoparticle solution. The bright areas are due to high electron density and thus indicate the presence of palladium. Right: graph showing the different metal affinities of seven different fungi. The fungi had been transferred into identically prepared colloidal solutions and grown for two months. The atomic fractions of metal:(metal+carbon) were obtained from EDX analysis.

Differences in the degree of occupation within one system can be attributed to morphological differences. By critical point drying of the hybrid systems, we were able to conserve the three-dimensional macroscopic shape.

The specific surface was estimated to be $0.4\ m^2\,g^{-1}$. First investigations exploring a potential application in catalysis were conducted on the potassium hexacyanoferrate(III) reduction via sodium thiosulfate and showed that the platinum nanocrystals retain catalytic activity when assembled onto the fungi.

Besides catalytic, electronic, or sensoric applications, the effect of nanoparticles assembling onto fungal mycelia could be a useful tool for biochemical investigations, for example, with regard to the heavy-metal accumulation effect. The nature of the chemical binding sites is thus of future interest.

Current investigations concentrate on the optimization of fungal surface coverage with nanoparticles with respect to the catalytic entity as well as the regaining of the noble metal. It will be investigated whether seeded growth of the assembled nanoparticles can lead to a tube system which is mechanically stable even after removal of the fungal template. Further studies will include other living entities, for example, yeast and bacteria.

Experimental Section

For experimental details please consult the Supporting Information.

Received: April 17, 2008
Published online: September 4, 2008

Keywords: catalysis · fungus · nanoparticles · template synthesis · transition metals

[1] G. Zeck, P. Fromherz, *Proc. Natl. Acad. Sci. USA* **2001**, *98*, 10457 – 10462.
[2] S. A. Davis, H. M. Patel, E. L. Mayes, N. H. Mendelson, G. Franco, S. Mann, *Chem. Mater.* **1998**, *10*, 2516 – 2524.
[3] V. Berry, S. Rangaswamy, R. F. Saraf, *Nano Lett.* **2004**, *4*, 939 – 942.
[4] V. Berry, A. Gole, S. Kundu, C. J. Murphy, R. F. Saraf, *J. Am. Chem. Soc.* **2005**, *127*, 17600 – 17601.
[5] a) Z. Li, S.-W. Chung, J.-M. Ginger, C. A. Mirkin, *Angew. Chem.* **2003**, *115*, 2408 – 2411; *Angew. Chem. Int. Ed.* **2003**, *42*, 2306 – 2309; b) N. L. Rosi, C. Shad Thaxton, C. A. Mirkin, *Angew. Chem.* **2004**, *116*, 5616 – 5619; *Angew. Chem. Int. Ed.* **2004**, *43*, 5500 – 5503.
[6] A. Sugunan, P. Melin, J. Schnürer, J. G. Hilborn, J. Dutta, *Adv. Mater.* **2007**, *19*, 77 – 81.
[7] a) A. Szeghalmi, S. Kaminskyj, P. Rösch, J. Popp, K. M. Gough, *J. Phys. Chem. B* **2007**, *111*, 12916 – 12924; b) K. Hering, D. Cialla, K. Ackermann, T. Dörfer, R. Möller, H. Schneidewind, R. Mattheis, W. Fritzsche, P. Rösch, J. Popp, *Anal. Bioanal. Chem.* **2008**, *390*, 113 – 124; c) P. Rösch, M. Harz, M. Schmitt, J. Popp, *J. Raman Spectrosc.* **2005**, *36*, 377 – 379.
[8] a) P. L. Freund, M. Spiro, *J. Phys. Chem.* **1985**, *89*, 1074 – 1077; b) Y. Li, J. Petroski, M. A. El-Sayed, *J. Phys. Chem. B* **2000**, *104*, 10956 – 10959.
[9] a) K. R. Brown, D. G. Walter, M. J. Natan, *Chem. Mater.* **2000**, *12*, 306; b) G. Frens, *Nature Phys. Sci.* **1973**, *241*, 20 – 22; c) J. Turkevich, J. Hillier, P. C. Stevenson, *Discuss. Faraday Soc.* **1951**, *11*, 55 – 75.

